

# Tin Dioxide Nanostructure Gas Sensor for Acetone and Methanol Detection

Osama Abdul Azeez Dakhil, Raad S. Sabry, Safaa Farhood Madlul  
Department of Physics, College of Science, Al-Mustansiriyah University, Iraq

## Article info

Received  
13/4/2016  
Accepted  
8/5/2016

## Keywords:

Nanostructure, gas sensor, screens print, thick films, simple evaporation.

## ABSTRACT

Simple and efficient technique were successfully used to prepare Tin dioxide ( $\text{SnO}_2$ ) nanostructure by simple evaporation method, using single stage horizontal tube furnace under atmosphere pressure and quartz tube with Argon flow without additive.  $\text{SnO}_2$  thick films were synthesized using simple, homemade, low-cost efficient screen print technique. The thick films were heated at  $500^\circ\text{C}$  for one hour to vanish the organic material and any residual impurities. The prepared thick films were investigated using different techniques and apparatus, X-Ray and FESEM to study the structural and morphology of the films, the X-ray results show that the films are polycrystalline with sharp and high intensity peaks indicating high crystallinity of the product. The FESEM Images show homogenous nanostructure with high porosity the dimension range 40-70 nm, optical properties was studied with photoluminescence emission (PL) and transmittance in UV-Visible range.  $\text{SnO}_2$  sensor was built up by electroding the thick films and used for Acetone and methanol detection.

## الخلاصة

تقنية غير معقدة وكفوءة تم استخدامها بنجاح لتحضير ( $\text{SnO}_2$ ) بتراكيب نانوية وذلك باستخدام تقنية التبخر البسيط باستخدام فرن انبوبي وانبوبة كوارتز وبوجود غاز الاركون وضمن الضغط الجوي بدون وجود عامل مساعد. تم تصنيع اغشية سميكة من ( $\text{SnO}_2$ ) باستخدام تقنية الطباعة على الشبكة وهي بسيطة وذات كلفة واطنة وفعالة، ان هذه الطريقة تعطينا اي تصميم او ابعاد للغشاء وبالتصاقية جيدة بين الغشاء والقاعدة. بعد ذلك تم تسخين الاغشية المحضرة لمدة ساعة وعند درجة حرارة 500 م للتخلص من الرابط العضوي واي شوائب اخرى. تم دراسة الخصائص التركيبية و دراسة السطح للاغشية المحضرة بفحصها ب باجهزة ال X-ray, FESEM حيث اظهرت فحوصات الحيود بالاشعة السينية ان الاغشية ذات تركيب متعدد التبلور مع قمم حادة ذات شدة عالية مما يدل على تبلور جيد للمادة، واظهرت صور المجهر الالكتروني الماسح تراكيب نانوية بابعاد تتراوح 40-70 نانومتر. وتم دراسة اخصاص البصرية للاغشية المحضرة من خلال فحص التألقية الضيائية (PL)، كذلك قياس النفوذية وفجوة الطاقة. تم بناء المتحسس الغازي بعد تقطير الاغشية وبنفس تقنية الطباعة على الشبكة وتم استخدامه للكشف عن الاسبينول والميثانول.

## INTRODUCTION

Evolution of methods for the controlled fabrication of nanostructures is currently the super goal in the domain of nanoscience and nanotechnology. Newly, much interest has been pointed to the use of low dimensional nanostructures such as nanoparticles, nanowires (NWs), and nanotubes, as building blocks in the production of hierarchical nanostructures because of different novel applications [1, 2, 3]. Researchers and scientists developed a techniques and methods to produce a wide range of different nanostructures. Hierarchical nanostructures based on NWs can be used as solar-cells, optoelectronic devices and gas sensors [5, 6, 7]. Due to characteristic high porosity of hierarchical nanostructures.

Precise detection of acetone and methanol scales in expel human breath, helping as breath indications for some diseases such as diabetes and mouth bad smell, may give useful information for early diagnosis of these diseases and environmental hazard. Using semiconductor metal oxide (SMO) gas sensors have attracted much attention due to low cost fabrication, miniaturization, and integration into portable devices [8, 9].

$\text{SnO}_2$  is an important semiconductor with a wide band gap. It has latent qualities can be utilized in many

applications and manufacturing optoelectronic devices such as gas sensors, photodetectors and solar cells. It's one of the important semiconductors that have been widely used for gas sensors. Since nanostructures such as nanowires, nanotubes, nanorods and nanoparticles have high surface to volume ratio [10, 11, 12], synthesis of these morphologies become the goal of researchers [13]. Recently,  $\text{SnO}_2$  nanostructures have been synthesized by different methods such chemical method, hydrothermal processing, thermal evaporation, spray pyrolysis and oxidation technique. In this work,  $\text{SnO}_2$  nanostructures synthesized successfully by the simple thermal reduction method with flow of argon and the product were investigated.

## MATERIALS AND METHODS

In simple thermal reduction synthesis method, a 80 cm long quartz tube with an inner diameter of 3 cm open on both sides one for Ar gas inlet and the other as excused was mounted inside a horizontal tube furnace. 99.99 % pure Sn powders were placed in an alumina boat ( $1 \times 1 \times 10 \text{ cm}^3$ ) positioned at the center of the quartz tube while pre cleaned Si substrate was placed in front of the boat,

the quartz tube was purged several times. The temperature in the tube furnace was rapidly raised up to 800 °C kept for 1 hour during the process, a steady flow of Ar gas (99.99 %) at a rate of 50 sccm was continued. The process continues for one hour then the furnace turn off to cool down. White powder was appears on the alumina boat and on the Si substrate. The product was collected carefully then thick films were made using efficient low coast screen print method, thick films were deposited on different substrates (Glass and p-type Si) the thickness was ranging between (3-4µm) to be characterized with different apparatus, the structural properties and morphology of the films by x-ray diffraction (XRD) using (*miniflex II Rigaku, Japan*) Cu K $\alpha$  radiation, field emission scanning electron microscopy (FESEM) (*Hitachi-S 4160-Japan*), optical properties and transmission measurements were carried out using a UV/visible spectrophotometer *Optima Sp-3000 plus UV-Vis-NIR (Split-beam Optics, Dual detectors)* in a range between 300 and 900nm. The PL spectra at room temperatures were achieved from 320 to 600nm using (*Perkin Elmer Spectrophotometer Luminescence LS 55 equipped with FL Win lab software*) with excitation wave length 280nm from Xenon lamp. To build the detector, a silver (IED) electrode was deposited on some of these films by screen print method. The sensing measurements were done using a homemade gas sensing system of 5000cm<sup>3</sup> chamber.

**RESULTS AND DISCUSSION**

The thick films were examined by (XRD) diffraction to study structural properties of the prepared films, Figure 1 shows polycrystalline structure with sharp peaks indicate high crystallinity, all the diffraction peaks refers to a rutile phase of SnO<sub>2</sub> according to JCPDS Card no. 411-445, (110), (101), (210), (211), no other peaks appears indicating high purity of the screen printed films. It's obvious from diffraction pattern the dominated growth with (110) plane. The crystallite size and structural parameters of the SiO<sub>2</sub> rutile phase estimated using Equations 1 and 2 [14, 15] respectively and extracted in Table 1:

$$D = \frac{0.9\lambda}{\beta \cos\theta} \tag{1}$$

Where D: crystallite size ,  $\lambda= 1.5406 \text{ \AA}$ ,  $\beta$ : the FWHM and  $\theta$ : the diffraction angle.

$$\frac{1}{d^2} = \frac{h^2}{a^2} + \frac{k^2}{b^2} + \frac{l^2}{c^2} \tag{2}$$

Table 1: Structural properties estimated from (XRD) pattern.

(hkl)	D (nm)	a, b (nm)	c (nm)
(110)	38	4.691	3.174
(101)	34	-	-
(210)	33	-	-

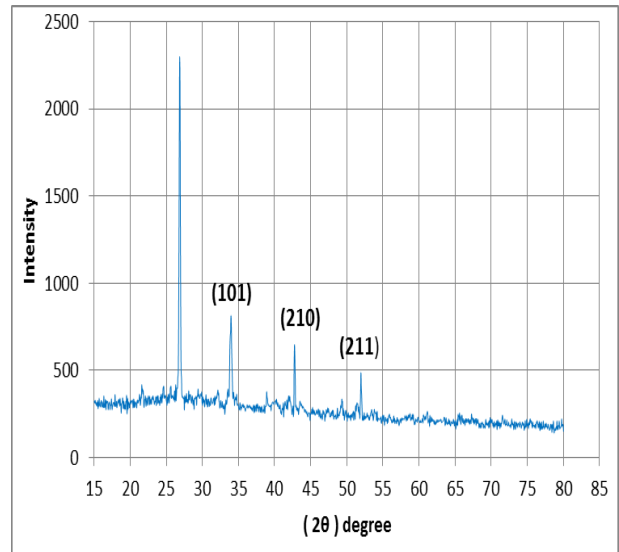
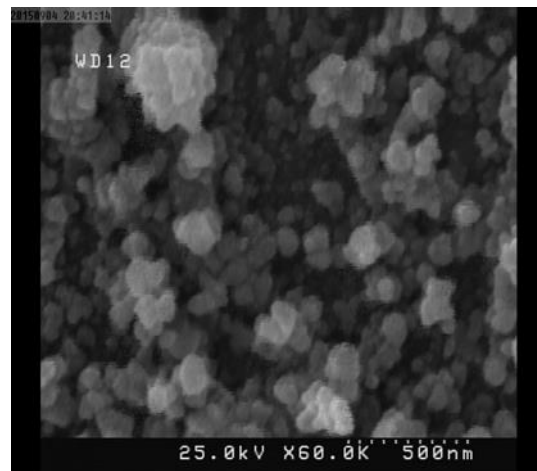


Figure 1: XRD diffraction of SnO<sub>2</sub> thick film.

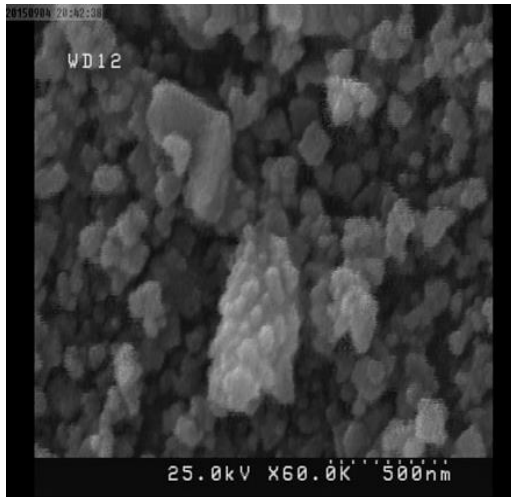
The morphology of the films was studied by FESEM, the pictures show homogeneous distribution with relatively high porosity due to deposition method. Also the grain size (Image J program) ranging between 40-70 (nm).



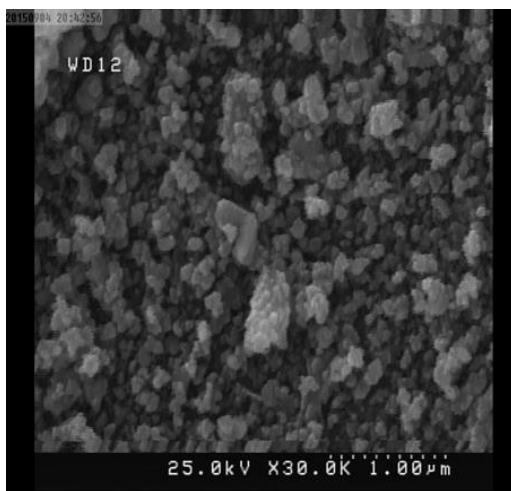
(a)



(b)



(c)



(d)

Figure 2: FESEM pictures for SnO<sub>2</sub> film.

The optical properties of the screen printed thick film deposited on a glass substrate were studied with UV–Visible light using shimatzu–visible spectrophotometer. The films show high transmittance in range between (350 -600) (nm) as shown in Figure 3.

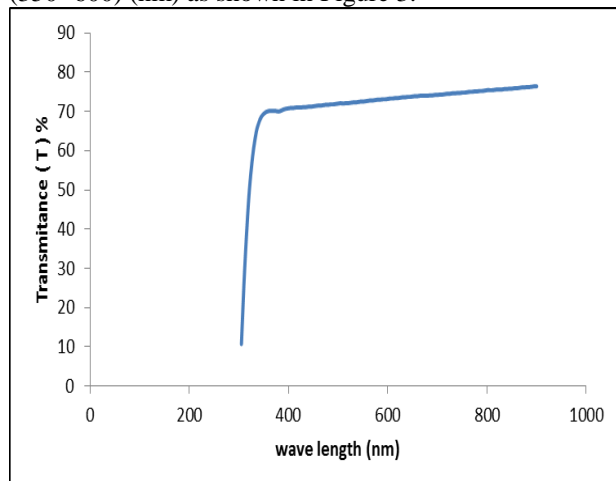


Figure 3: Transmission VS wave length.

The optical transition of SnO<sub>2</sub> crystals is known to be a direct transition so the absorption coefficient  $\alpha$  is obeys the relation [16]:

$$\alpha(h\nu) \propto (h\nu - E_g)^{1/2}/h\nu$$

Plots of  $(\alpha(h\nu))^2$  versus  $h\nu$  can be obtained from the data as shown in figure 4 The intercept of the tangent to the plot gives approximated value of the energy gap of the direct band gap materials it was found 3.83eV.

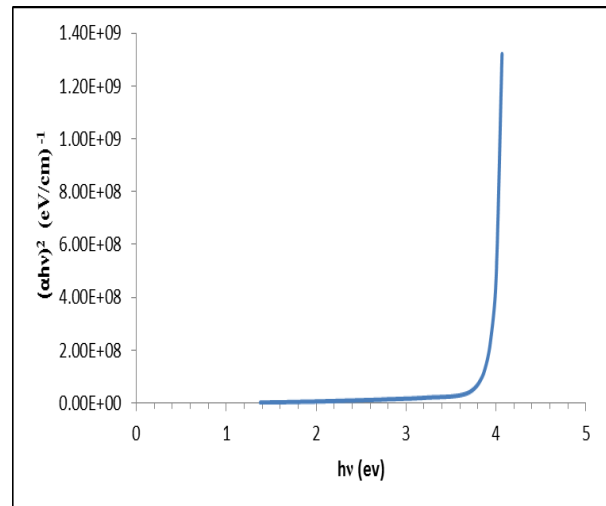
Figure 4:  $(\alpha h\nu)^2$  as a function of photon energy for SnO<sub>2</sub> thick films.

Figure 5 shows the variation of photoluminescence emission intensity of SnO<sub>2</sub> with energy of illumination wave length, a strong green emission band was observed around 518 nm with an energy gap of 2.39 eV This emission is refer to the crystal defects or the electron transition occurs by defect levels such as oxygen vacancies, tin interstitials and so on in the band gap during the growth, oxygen vacancies are known to be the major defects and usually act as radiative positions in luminescence processes The oxygen vacancies existing in three different charge states  $V_o^0$ ,  $V_o^+$  and  $V_o^{++}$  in the semiconductor oxides [17, 18]. As  $V_o^0$  is a very thin donor, the most oxygen vacancies will be in their paramagnetic  $V_o^+$  state under thick-band conditions. Hence, the origin of the green emission band in the PL spectrum of SnO<sub>2</sub> nanostructure is because of the recombination process of electrons in the singly occupied oxygen vacancies with photo excited holes in the valance band vacancies. In the present SnO<sub>2</sub> nanostructure, the defects, such as oxygen vacancies, it act as luminescent positions, forming defect levels lying highly in the gap, attract electrons from the valance band enhance the luminescence [19].

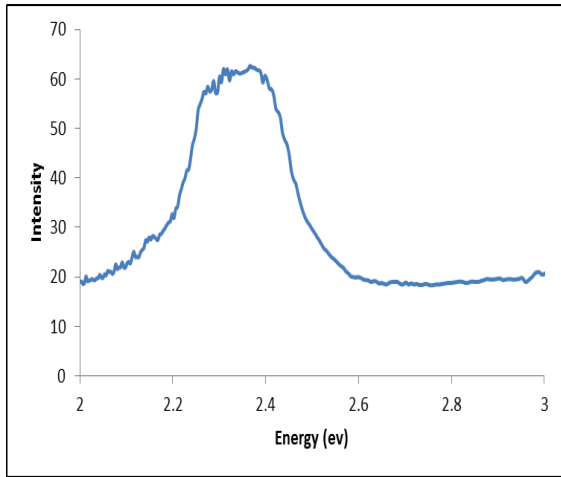


Figure 5: Room Temperature PL of SnO<sub>2</sub> Thick Film.

After film characterization the sensor was synthesized by electroding it with silver (IDE) electrode using screen prints method. The sensor exposure for different concentrations of Methanol Figure 6 and Acetone Figure 7 inside the chamber, the sensor shows higher sensitivity for Acetone and relatively faster response and recovery comparing with Methanol [20]. Also the operating temperature was investigated for both Acetone and Methanol; the obtained results were illustrated in Table 2.

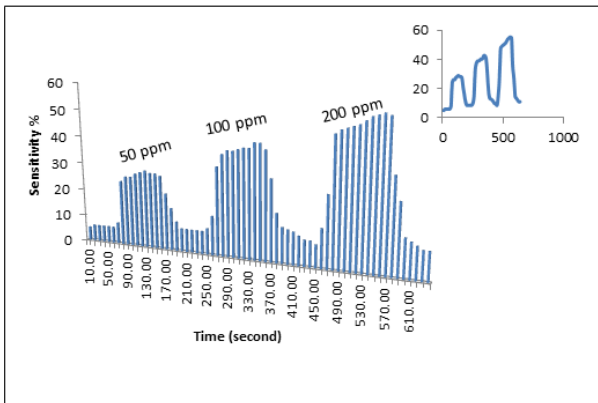


Figure 6: Change of Sensitivity of SnO<sub>2</sub> thick film with time for different concentrations of methanol.

Table 2: Response, recovery, and operating temperature of Acetone and Methanol.

Gas	Response time(sec)	Recovery time( sec)	Operating temperature
Methanol	80	110	200 <sup>o</sup> C
Acetone	60	90	175 <sup>o</sup> C

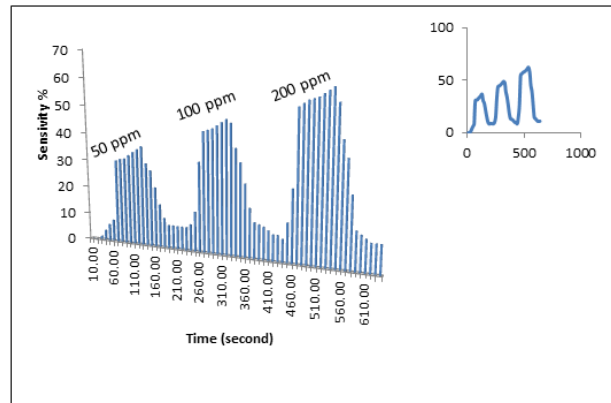


Figure 7: Change of Sensitivity of SnO<sub>2</sub> Thick Film with time for different concentrations of Acetone.

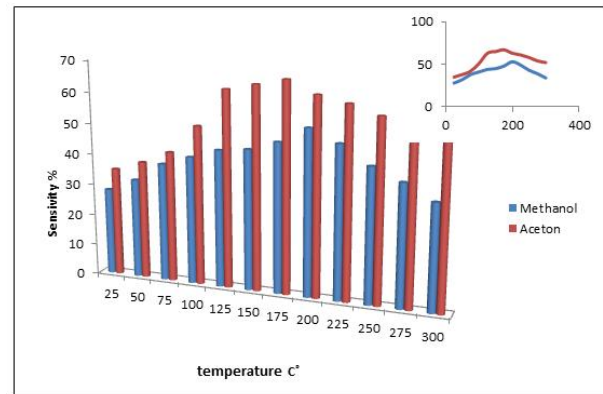


Figure 8: Change of Sensitivity of SnO<sub>2</sub> Thick Film with temperature at 100 ppm of Acetone and Methanol.

### CONCLUSIONS

In summary, SnO<sub>2</sub> nanostructures were synthesized from Sn powder by simple evaporation method with Ar gas flow at atmospheric pressure. The temperature in the furnace was rapidly raised up to 800 °C kept for 60 min. The optical direct band gap estimated its found around 3.8eV. The microstructures of the SnO<sub>2</sub> nanowires were characterized. The morphology of the products depends on the preparation conditions (flow rate, temperature and heating time). The room temperature PL spectra of the SnO<sub>2</sub> nanostructure with high porosity screen print film showed a strong green band emission at 518nm with a band gap of 2.39eV, which is connected with oxygen vacancies or surface defect states, sensing parameters for Acetone and Methanol were estimated. The results indicate it is promising for use in sensing devices.

### REFERENCES

- [1] L. C. Nehru, V. Swaminathan, C. Sanjeeviraja, "Photoluminescence Studies on Nanocrystalline Tin Oxide Powder for Optoelectronic Devices", American Journal of Materials Science 2 (2), pp. 6-10, 2012.
- [2] Suhua Luo, Jiyang Fan, Weili Liu, MiaoZhang, ZhitangSong, Chenglu Lin, XinglongWu and Paul

- KChu, "Synthesis and low-temperature photoluminescence properties of SnO<sub>2</sub> nanowires and nanobelts", *Nanotechnology* 17, pp.1695–1699, 2006.
- [3] Shuhui Sun, Guowen Meng, Gaixia Zhang, and Lide Zhang, "Controlled Growth and Optical Properties of One-Dimensional ZnO Nanostructures on SnO<sub>2</sub> Nanobelts", *Crystal Growth and Design*, Vol. 7, No. 10, pp.1989-1991, 2007.
- [4] Paulo G. Mendes, Mario L. Moreira, Sergio M. Tebcherani, Marcelo O. Orlandi, J. Andre´s, Maximu S. Li, Nora Diaz-Mora, Jose´ A. Varela, Elson Longo, "SnO<sub>2</sub> nanocrystals synthesized by microwave-assisted hydrothermal method: towards a relationship between structural and optical properties", *J Nanopart Res* pp.14-750, 2012.
- [5] Toshinari Yamazaki, "Formation of Oxide Nanowires by Thermal Evaporation and Their Application to Gas Sensors", *Nanowires – Implementations and Applications*, [www.intechopen.com](http://www.intechopen.com), pp. 117-140, 2011.
- [6] Sumanta Kumar Tripathy, "Optical and Structural Characteristics of Copper Doped Tin Oxide Thin Film Prepared by Thermal Evaporation Method", *International Journal of Engineering and Innovative Technology (IJEIT)* Volume 3, Issue 1, July 2013.
- [7] T. Tharsika, A. S. M. A. Haseeb, Sheikh A. Akbar, Mohd Faizul Mohd Sabri and Wong Yew Hoong, "Enhanced Ethanol Gas Sensing Properties of SnO<sub>2</sub>-Core/ZnO-Shell Nanostructures", *Sensors* 14, pp.14586-14600, 2014.
- [8] C M Liu, XTZu, QMWei and L M Wang, "Fabrication and characterization of wire-like SnO<sub>2</sub>", *J. Phys. D: Appl. Phys.* 39, pp.2494–2497, 2006.
- [9] Feng Yang Kai, Huang Shibing Ni, Qi Wang Deyan He, "W18O49 Nanowires as Ultraviolet Photodetector", *Nanoscale Res Lett* 5, pp.416–419, 2010.
- [10] Le Viet Thong, Le Thi Ngoc Loan, Nguyen Van Hieu, "Comparative study of gas sensor performance of SnO<sub>2</sub> nanowires and their hierarchical nanostructures", *Sensors and Actuators B* 150, pp.112–119, 2010.
- [11] Rui Chen, G. Z. Xing, J. Gao, Z. Zhang, T. Wu and H. D. Sun, "Characteristics of ultraviolet photoluminescence from high quality tin oxide nanowires", *Appl. Phys. Lett.* 95, 061908., 2009.
- [12] Le Duy Khanh, Nguyen Thanh Binh, Le Thi Thanh Binh and Nguyen Ngoc Long, "SnO<sub>2</sub> Nanostructures Synthesized by Using a Thermal Evaporation Method", *Journal of the Korean Physical Society*, Vol. 52, No. 5, pp. 1689-1692, May 2008.
- [13] S. Morrison, Selectivity in semiconductor gas sensors, *Sensors and Actuators, B* (12), pp. 425-440, 1987.
- [14] H. Pulker, Characterization of optical thin film, *Applied Optics*, 18, pp. 1969, 1979.
- [15] Ganesh E Patil, Dnyaneshwar D Kajale, Vishwas B Gaikwad and Gotan H Jain, "Preparation and characterization of SnO<sub>2</sub> nanoparticles by hydrothermal route", *International Nano Letters* pp. 2:17, 2012.
- [16] V. Kumar, D.K. Dwivedi, P. Agrawal, "Optical, Structural and Electrical Properties of Nanosized Zinc Oxide Sintered Films for Photovoltaic Applications", *Science of Sintering*, 45, pp.13-19, 2013.
- [17] E. P. Domashevskaya, N. M. A. Hadia, S. V. Ryabtsev, P. V. Seredin, "Structure and photoluminescence properties of SnO<sub>2</sub> nanowires Synthesized from SnO powder", *КОНДЕНСИРОВАННЫЕ СРЕДЫ И МЕЖФАЗНЫЕ ГРАНИЦЫ*, Том 11, № 1, 2009.
- [18] B. Wang, I.L. Li, P. Xu and L.W. Xing, "Fabrication and Photoluminescence of Plate-Shape OF the SnO<sub>2</sub> Nanostructures", *Rev. Adv. Mater. Sci.* 33, pp.164-170, 2013.
- [19] Yung-Chiun and Jer-Yau Wu, "Low-temperature growth and blue luminescence of SnO<sub>2</sub> nanoblades", *Applied Physics Letters* 89, 043115, 2006.
- [20] Seon-Jin Choi, Bong-Hoon Jang, Seo-Jin Lee, Byoung Koun Min, Avner Rothschild, and Il-Doo Kim, "Selective Detection of Acetone and Hydrogen Sulfide for the Diagnosis of Diabetes and Halitosis Using SnO<sub>2</sub> Nanofibers Functionalized with Reduced Graphene Oxide Nanosheets", *Appl. Mater. Interfaces* 6, pp. 2588–2597, 2014.